AFOSR-TR-97

REPORT DOCUMENTATION PAGE

0577

1. AGENCY USE ONLY (Leave blank)	2. REPORT DATE	3. REPORT TYPE AND DATES COVERED
		FINAL REPORT - 01 Aug 93 - 31 July 97

4. TITLE AND SUBTITLE
(AASERT-93) MICROWAVE ABSORPTION AND REFLECTION FROM ULTRAVIOLET LASER AND ELECTRON CYCLOTRON RESONANCE PRODUCED PLASMAS

5. FUNDING NUMBERS
61103D
3484/TS

6. AUTHOR(S)
Professor John E. Scharer

7. PERFORMING ORGANIZATION NAME(S) AND ADDRESS(ES)
Dept of Electrical and Computer Engineering
University of Wisconsin-Madison
1415 Engineering Drive
Madison, WI 53706-1691

8. PERFORMING ORGANIZATION REPORT NUMBER

9. SPONSORING/MONITORING AGENCY NAME(S) AND ADDRESS(ES)
AFOSR/NE
110 Duncan Avenue Suite B115
Bolling AFB DC 20332-8050

10. SPONSORING/MONITORING AGENCY REPORT NUMBER
F49620-93-1-0465

11. SUPPLEMENTARY NOTES

12a. DISTRIBUTION/AVAILABILITY STATEMENT
APPROVED FOR PUBLIC RELEASE: DISTRIBUTION UNLIMITED

12b. DISTRIBUTION CODE

13. ABSTRACT

This report contains information regarding progress on experiments associated with microwave reflection, absorbtion, and transmission with a laser produced plasma sheet. The progress report is in response to AFOSR AASERT Award F49620-93-1-0465.

The objective of this research is to create a laser produced plasma with a high enough density to reflect or absorb microwaves. The plasma acts as an inertialess reflective or absorptive surface which can be used as an agile mirror in the reflective case, or as a cloaking shield in the absorptive case.

During the past year a new laser was purchased to assist in the research. The new laser installation was accomplished in August 1996. A new heterodyne detection system was also studied to see its benefits as compared to a homodyne system used previously. The National Instruments data acquisition package LabView 4.0.1 was purchased for better interaction with Tektronix oscilliscopes. A new LabView driver was programmed into an updated PowerMac computer.

14. SUBJECT | **NUMBER OF PAGES**

PRICE CODE

17. SECURITY CLASSIFICATION OF REPORT	18. SECURITY CLASSIFICATION OF THIS PAGE	19. SECURITY CLASSIFICATION OF ABSTRACT	20. LIMITATION OF ABSTRACT
UNCLASSIFIED	UNCLASSIFIED	UNCLASSIFIED	

Final Report for AFOSR AASERT Award F49620-93-1-0465

Microwave Absorption, and Reflection from Ultraviolet Laser and Electron Cyclotron Resonance Produced Plasma Sheet

Kurt L. Kelly
Under the Supervision of Professor John E. Scharer
Department of Electrical and Computer Engineering
University of Wisconsin–Madison
Madison, Wisconsin 53706

January 1997

1 Introduction.

This report contains information regarding progress on experiments associated with microwave reflection, absorbtion, and transmission with a laser produced plasma sheet. The progress report is in response to AFOSR AASERT Award F49620-93-1-0465.

The objective of this research is to create a laser produced plasma with a high enough density to reflect or absorb microwaves. The plasma acts as an inertialess reflective or absorptive surface which can be used as an agile mirror in the reflective case, or as a cloaking shield in the absorptive case.

During the past year a new laser was purchased to assist in the research. The new laser installation was accomplished in August 1996. A new heterodyne detection system was also studied to see its benefits as compared to a homodyne system used previously. The National Instruments data acquisition package LabView 4.0.1 was purchased for better interaction with Tektronix oscilliscopes. A new LabView driver was programmed into an updated PowerMac computer.

2 Theory of Electromagnetic Propagation Through a Plasma.

This section presents a theoretical model of propagation of plane waves through a plasma. The dispersion relation for plane wave propagation in a plasma is

$$k_p^2 c^2 = \omega^2 - \frac{\omega \omega_{pe}^2}{\omega + j\nu} \tag{1}$$

in which ω_{pe} is defined as the electron plasma frequency

$$\omega_{pe}^2 = \frac{e^2 n_e}{m_e \epsilon_o} \tag{2}$$

and ν is the electron-neutral collision frequency. The complex propagation constant k is defined as

$$k_p = \beta_p + j\alpha_p \tag{3}$$

The wave attenuates according to α_p and propagates according to β_p. Inserting (3) into (1) a complex equation results which relates α_p and β_p to ω_{pe}

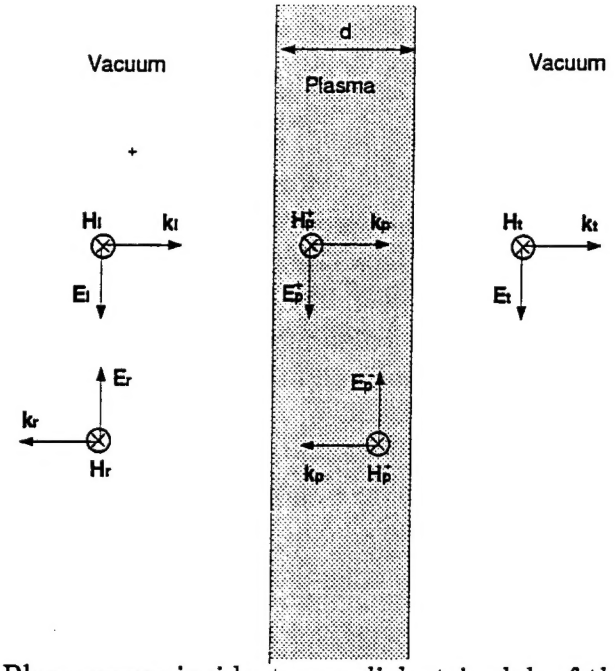

Figure 1: Plane waves incident on a dielectric slab of thickness d.

and ν. If α_p and β_p can be found then ω_{pe} and ν can also be found. The required complex equation is

$$\beta_p^2 - \alpha_p^2 + j2\alpha_p\beta_p = \frac{\omega^2}{c^2} - \frac{\omega_{pe}^2}{c^2}\frac{\omega(\omega - j\nu)}{\omega^2 + \nu^2} \tag{4}$$

2.1 Dielectric Slab Model

Propagation of plane electromagnetic waves through a dieletric slab of thickness d is illustrated in Figure 1. By matching boundary conditions at 0 and d and solving for the ratios of incident, reflected and transmitted power, power refection and transmission coefficients are obtained [1]

$$R = rr^* = \frac{sin^2\beta_p d + sinh^2\alpha_p d}{sin^2(\beta_p d + \theta) + sinh^2(\alpha_p d + S)}, \tag{5}$$

$$T = tt^* = \frac{sin^2\theta + sinh^2 S}{sin^2(\beta_p d + \theta) + sinh^2(\alpha_p d + S)}, \tag{6}$$

in which

$$r_s = \frac{(\beta_o - \beta_p)^2 + \alpha_p^2}{(\beta_o + \beta_p)^2 + \alpha_p^2}, \tag{7}$$

$$\phi_{r_s} = tan^{-1}\frac{-2\beta_o\alpha_p}{\beta_o^2 - \beta_p^2 - \alpha_p^2}, \tag{8}$$

and

$$S = -\frac{1}{2}ln(r_s), \tag{9}$$

and in which r_s and ϕ_{r_s} are the magnitude and angle, respectively, of the reflection coefficient for a single free space — plasma interface. The subscript "s" on ϕ_r indicates "single interface", and ϕ_R denotes the reflected phase shift with no such restriction.

There are now four equations in six unknowns — α_p, β_p, n_e, ν_e, T and R. By measuring any two of the unknowns, all the others can be determined. Measuring R and T and solving for α_p and β_p makes the numerical difficulty considerably greater than measuring β_p and T or β_p and R and then solving for α_p. At present it is planned to measure β_p and T, solve for α_p using (6) and then solve for n_e and ν using (4).

2.2 The Budden Model

Although the dielectric slab description is accurate for a homogeneous plasma, it was determined that there were several areas that this model was innacurate. Several different values of density would yeild a dielectric constant which allowed a large amount of radiation to tunnel through the plasma. The plasma could be thought of as a lossy dielectric slab. Since this phenomena wasn't observed in the lab a better approximation was sought. In experiments by Shen, Scharer, Porter, Lam and Kelly [2], the plasma was determined to not have a step profile as in the dielectric slab, but rather a peak density near it's center, with a somewhat less dense plasma near it's edge. Budden has solved the wave equation for a dielectric with just such a profile. It was determined that this Epstein profile more accurately described the real phenomena we were looking at. This theory gave a closed form solution for the reflected and transmitted waves and could account for different densities as well as a wide range of collision frequencies. Either low loss reflection or highly lossy absorbers can be treated with this formalism.

The Budden Model is based on a solution to the hypergeometric equation:

$$\zeta(1-\zeta)(\frac{d^2u}{d^2\zeta}) + \{c-(a+b+1)\zeta\}\frac{du}{d\zeta} - abu = 0 \tag{10}$$

If we let

$$-\zeta = e^{\mathcal{Z}} \tag{11}$$

and

$$\mathcal{Z} = (z/\sigma) \tag{12}$$

the hypergeometric equation is transformed into:

$$(1+e^{\mathcal{Z}})\frac{d^2u}{d^2\mathcal{Z}} + \{c-1+(a+b)e^{\mathcal{Z}}\}\frac{du}{d\mathcal{Z}} + abe^{\mathcal{Z}}u = 0 \tag{13}$$

This is transformed into its normal form by substituting

$$u = Eexp\{\frac{1}{2}(1-c)(\mathcal{Z})\}(1+e^{\mathcal{Z}})^{(\frac{c-1-a-b}{2})} \tag{14}$$

where E will be used to denote the electric field. We now obtain the wave equation:

$$\frac{d^2E}{d^2z} + k^2q^2E = 0 \tag{15}$$

where

$$q^2 = \epsilon_1 + \frac{e^z}{(e^z+1)^2}\{\epsilon_2-\epsilon_1)(e^z+1)+\epsilon_3\} \tag{16}$$

and

$$\epsilon_1 = -\frac{1}{4}\frac{(c-1)^2}{\sigma^2k^2} \tag{17}$$

$$\epsilon_2 = \frac{1}{4}\frac{(a-b)^2}{\sigma^2k^2} \tag{18}$$

$$\epsilon_3 = \frac{1}{4}\frac{(a+b+1-c)(a+b-1-c)}{\sigma^2k^2} \tag{19}$$

If we substitute the following parameters for a, b, and c:

$$c-1 = -2ik\sigma cos^2(\theta) \tag{20}$$

$$a-b = -2ik\sigma q_0 \tag{21}$$

$$a+b-c = \pm(4k^2\sigma^2\epsilon_3+1)^{\frac{1}{2}} \tag{22}$$

we get a closed form solution of the wave equation for the reflected and transmitted waves.

It can be seen that if we let

$$\epsilon_1 = \epsilon_2 = cos^2\theta \tag{23}$$

and

$$\epsilon_3 = \frac{-4X_m}{1 - iZ} \tag{24}$$

we get a dielectric constant of a plasma with density profile given by

$$X = X_m sech^2(\frac{z}{2\sigma}) \tag{25}$$

and a collisonality given by

$$Z = \frac{\nu}{\omega} \tag{26}$$

The parameter σ can be thought of as a thickness parameter. The reflection and transmission coefficients become

$$R = \frac{(-2ik\sigma Cos\theta)!(2ik\sigma Cos\theta - \gamma - \frac{1}{2})!(2ik\sigma Cos\theta + \gamma - \frac{1}{2})!}{(2ik\sigma Cos\theta)!(-\gamma - \frac{1}{2})!(\gamma - \frac{1}{2})!} \tag{27}$$

and

$$T = [2ik\sigma Cos(\theta)]\frac{[2ik\sigma Cos(\theta) - \gamma - \frac{1}{2}]![2ik\sigma Cos(\theta) + \gamma - \frac{1}{2}]!}{[2ik\sigma Cos(\theta)!]^2} \tag{28}$$

where

$$4\gamma^2 = 1 + 4k^2\sigma^2\epsilon_3 \tag{29}$$

A computer code was developed to interpret results of Epstein profiles and to optimize the experimental conditions. A study of figure 2 determined that at a 9 GHz operating frequency, it was desirable to have a sharp boundary to produce a highly reflective plasma. This is consistant with the slab model. An exmaination of figure 3, meanwhile, suggested a more diffuse boundary could produce result in a highly absorptive plasma. Another important parameter is the collision frequency. Operating at higher neutral pressures could enhance the absorptive properties of the plasma as this would provide a larger neutral density. Also, backfilling the chamber with an inert gas such as argon could lessen the effects of collsionality by decresing the number of negative ions in the plasma.

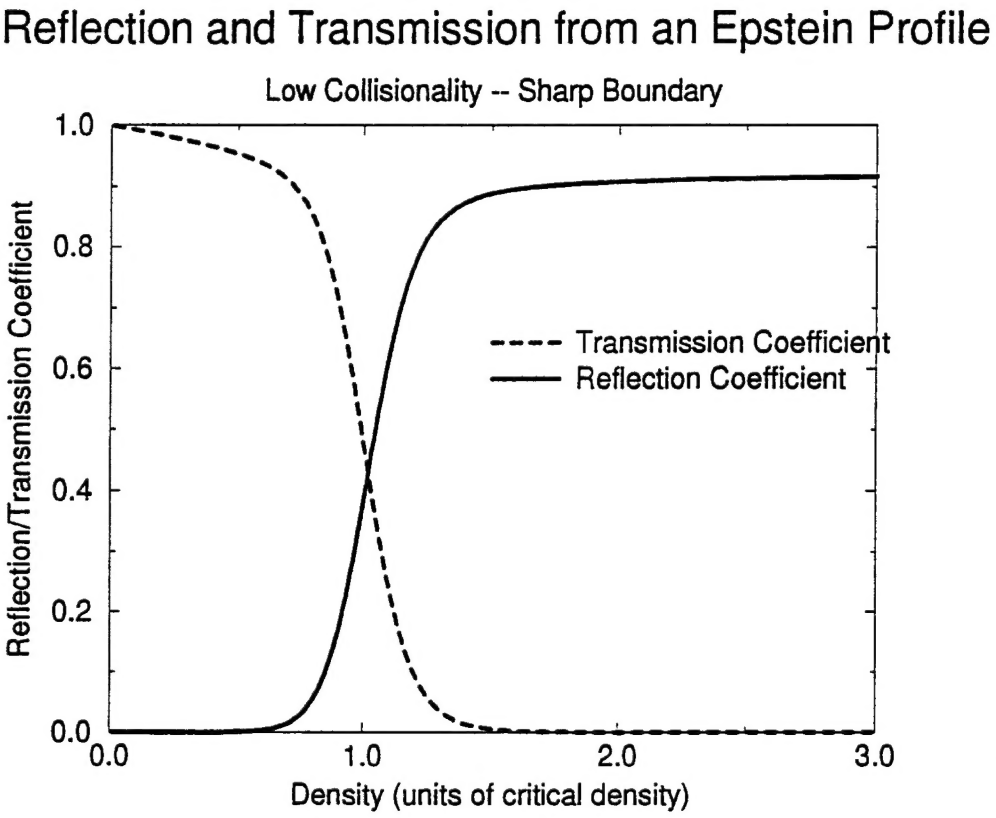

Figure 2: A sharp boundary ($\sigma = 1cm$) slightly collisional ($\nu = 90MHz$) sheet can be highly reflective if it has adequate plasma denstiy.

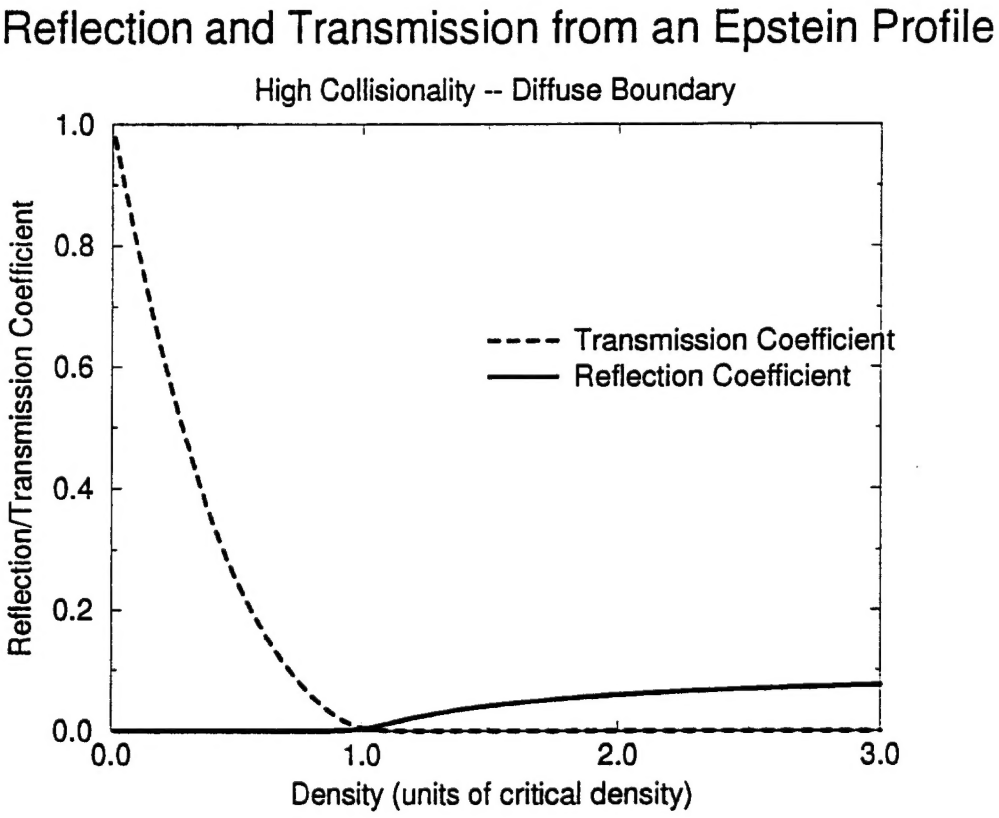

Figure 3: A diffuse boundary ($\sigma = 10cm$) highly collisional ($\nu = 1GHz$) sheet can be highly absorptive even at low plasma density.

3 Purpose.

Radar scanning can be carried out in a number of ways. A most simple example is a single element transmitter scanned mechanically in elevation and azimuth. Such a radar system might work in a few applications in which objects are moving very slowly, or are very far away (astronomical distances). But for most applications, such as for tracking aircraft or missiles, a mechanical scanner is far too slow.

Another way of radar scanning is the use of a phased array. In this case, an array of individual radiating elements are excited with differing phases controlled such that a narrow beam can be scanned. They have no moving parts. Phased arrays have been used for decades in radar applications. They are fast and effective in determining the location and velocity of objects. However they are very large and require large amounts of power and microwave circuitry to operate. For use on mobile crafts such as a warship, they can be cumbersome.

This report describes some basic research aimed at using a single element horn antenna as a source , reflecting it off a planar plasma sheet for scanning purposes, and yet avoiding the disadvantages of a mechanical moving device. The idea is to optically rotate a plasma reflector. Various methods may be used to rotate the plasma refector. Researchers at the Naval Research Laboratory use an array of hollow cathodes to start a planar gas discharge. The planar discharge is rotated by applying voltage to a set of electrodes [3]. Another method of rotating a plasma is to generate it with a short pulse laser beam, wait for the ions and electrons to recombine, electrically rotate the laser beam, and then generate a new plasma with another short pulse at the rotated position. The technology for rotating a laser beam exists commercially in the visible spectrum.

In addition, a highly collisional, diffuse plasma can be used for the absorbtion of microwaves. This is useful to reduce the radar cross-section of targets, essentially hiding them from radar detection systems.

This report considers the feasibility of the laser plasma generation scheme following the work of Shen and Scharer [2] and Zhang and Scharer [4]. It considers properties of the plasma and their effects on its ability to reflect microwave radiation in the X-band.

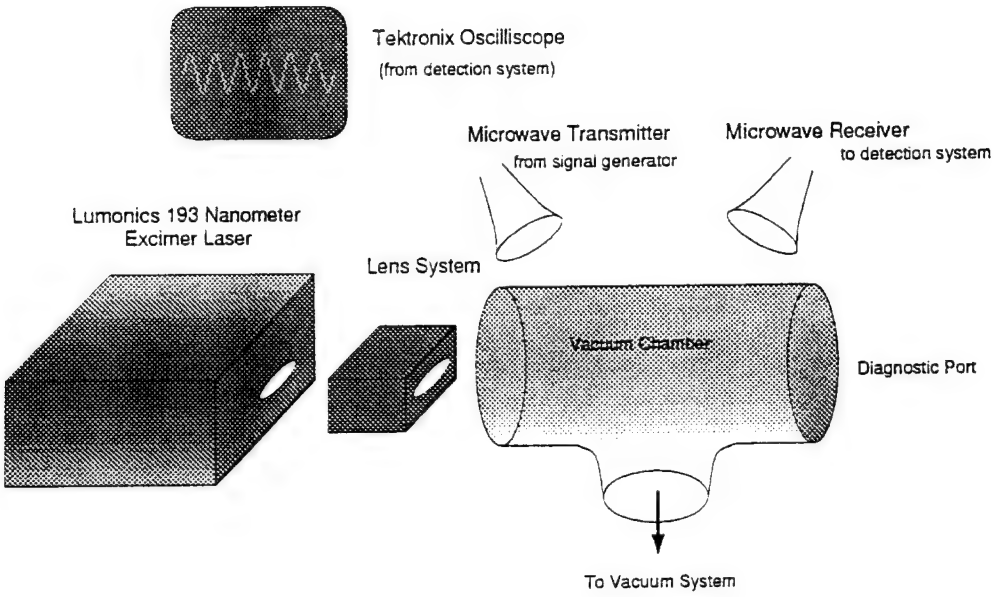

Figure 4: Laser-Plasma Microwave Radar Facility in 321ERB at the University of Wisconsin - Madison.

4 Description of the Laboratory and Experimental Conditions.

The experiment is being conducted at the University of Wisconsin-Madison. The laser radiation is directed into a vacuum chamber containing the organic gas Tetrakis(dimethyl-amino)ethylene (TMAE). The laser ionizes the gas creating a plasma. X-band microwaves are launched from a highly directive horn antenna toward the plasma where they will be partially transmitted and partially reflected. A bi-static antenna system was used for the purposes of isolation.

4.1 High Energy Excimer Laser Acquisition and Installation.

A new pulsed Ultra-Violet laser was purchased in the summer of 1996. This new laser can produce 300 mJ of VUV laser radiation. This represents a 200 fold improvement in laser power over a laser that was formerly utilized in this lab. The laser has stable output with only 5% shot-to-shot variation. This will make the results of the experiment much more repeatable than in the past. The laser was installed in June 1996. It has a water cooled system to regulate internal vessel pressure and temperature. A new filtration system was needed to provide sufficient water pressure while eliminating corrosive contaminents in the universty water system. The vessel contains a misture of four gases. Hydrogen is used to passivate the system after it has been exposed to atmosphere. The working gas mixture is a combination of Neon, Flourine, and Argon. The Flourine is combined with inert Helium in the supply tank for safety purposes. All gas purities are Ultra-High for superior laser performance. A new gas handling system was installed at the same time as the laser to insure sterility.

The laser power supply is contained in the main housing. It was neccesary to construct a reinforced table to support the 200 kg unit. Power is supplied by a 3 phase cable 110 Volts / phase capable of delivering 20 amps. The laser is capable of a 20 Hz repetition rate. Output energy is regulated by an internally calibrated photo-diode. Capacitor voltages and filling pressures are adjusted by internal feedback systems to ensure stable output.

The excimer laser is being operated at 193 nm with the use of Argon Flouride. Some of this energy is lost in the UV windows and O_2 absorption in air. Our preliminary measurements show that 5% of the radiation is lost to the windows. Further experiments have suggested that the laser energy decreases by 1.5 db / meter due to oxygen absorption. We are in the process of making a vacuum compatible channel which can be filled with an inert gas to reduce these losses and therefore utilize more of the available laser energy.

4.2 Lenses and Vacuum Chamber.

Most of the laser beam is contained in a region 7 $\times$ 20 mm at the laser output window. With a series of four custom design and fabricated Suprasil lenses manufactured by Midwest Optics, the laser beam can be adjusted to be (3-7)mm $\times$ (2-11)cm. Figure 5 is a diagram illustrating the lenses set to

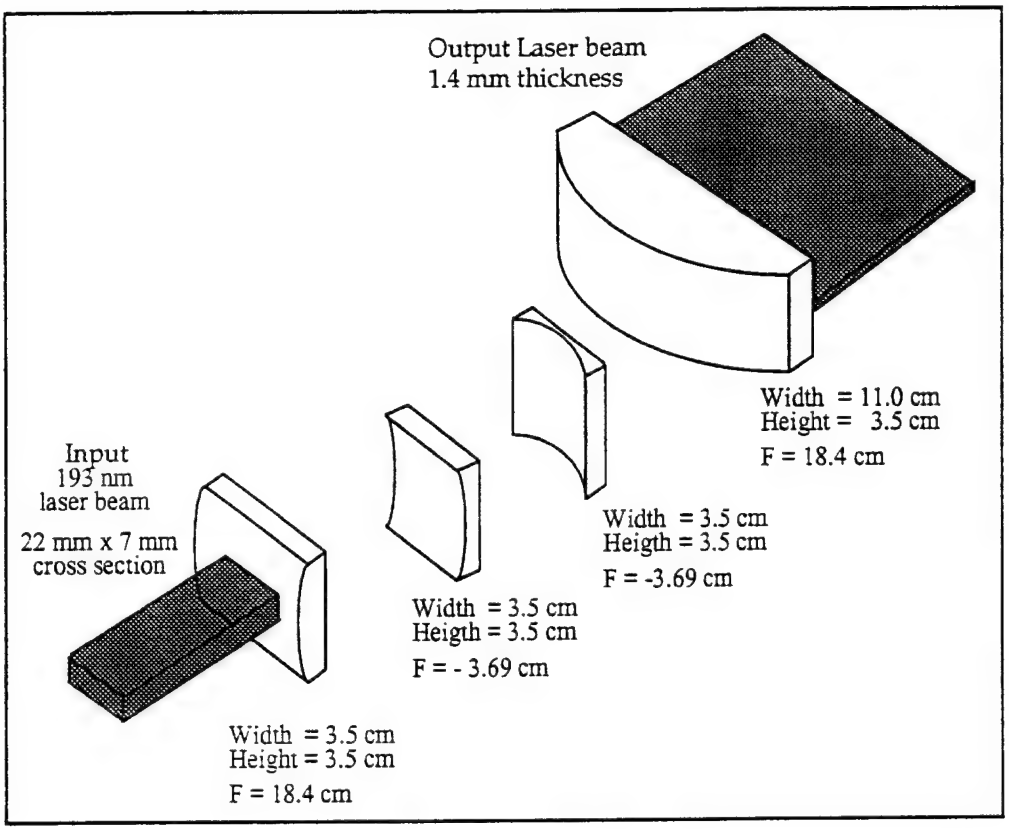

Figure 5: Suprasil lenses with VUV transmissive coating.

generate a 2 mm $\times$ 11 cm beam. The lenses are located in an aluminum box near the laser output window. It is hoped that the new channel will extend the lifetime of these lenses. It was determined that a typical lens has a 2-6 year lifetime due to degradation of the VUV coating. With the new higher power laser, this degradation has been observed. An aperture located between the third and fourth lenses - referenced from the laser side - can make the beam sharp in the y-direction. This is desirable because stray light outside the main laser beam can cause the plasma to be underdense in the region above and below the main plasma sheet. A sharp plasma boundary is desirable so as to approximate a piece of sheet metal. Approximating a sheet of metal is desirable since metal will be used as a 100% amplitude and 180^0 phase reflection reference.

The vacuum chamber is a 6 inch Corning glass T which is evacuated to

$10^{-}6$ Torr. This ensures TMAE vapor purity. The vapor pressure of TMAE is 350 mTorr at room temperature. Typical filling pressures are 60 - 100 mTorr. A new chamber was construçted by University of Wisconsin Phyical Science Labs in Septemer 1995 which will allow for microwave windows. The new chamber is constructed of steel. Several layers of absorptive paint will be applied to reduce extraneous reflections. The chamber was designed such that it can be supported and utilized with minimum reflections from vacuum pumps and other instrumentation which would normally interfere with accurate measurements.

4.3 Plasma Conditions.

The first ionization potential of TMAE is 5.36 eV. A photon of wavelength 193 nm has an energy of 6.40 eV. Consequently, for single photon ionization, an electron temperature of about 1eV can be expected initially. It is expected that collisions will reduce this value after a laser pulse has ended. Langmuir triple probe measurements [5] indicate that this is the case.

The plasma profile in the y-direction was measured with a planar circular disk Langmuir probe. A typical profile is shown in Figure 6. This profile was done with the aperture adjusted to 6mm and the lenses adjusted as shown in Figure 5. For these measurements, a reference probe was place near the laser beam and left in a constant position while a mobile probe was scanned in the y-direction.

4.4 Microwave Homodyne Detection System.

This section presents the microwave waveguide circuit used to measure the reflection off of and the transmission through the plasma. It also includes general theory of detection and how it is applies to the circuit.

4.4.1 Components.

Figure 7 shows the waveguide system designed to measure the amplitude and phase of the transmitted signal and reflected signals. All experiments were done with X-band microwaves using an HP Model 620A SHF Signal Generator. This is a tunable source with a peak output of about 100mW of power. For frequency measurements more accurate than the generator dial could indicate, an HP model 532B Frequency Meter was used. It was

Hyperbolic Secant Squared Profile

Thickness of profile is governed by parameter σ.
A diffuse boundary corresponds to a large value of σ.
A somewhat sharper boundary is characterized by a smaller value of σ. An actual density profile is shown for comparison.

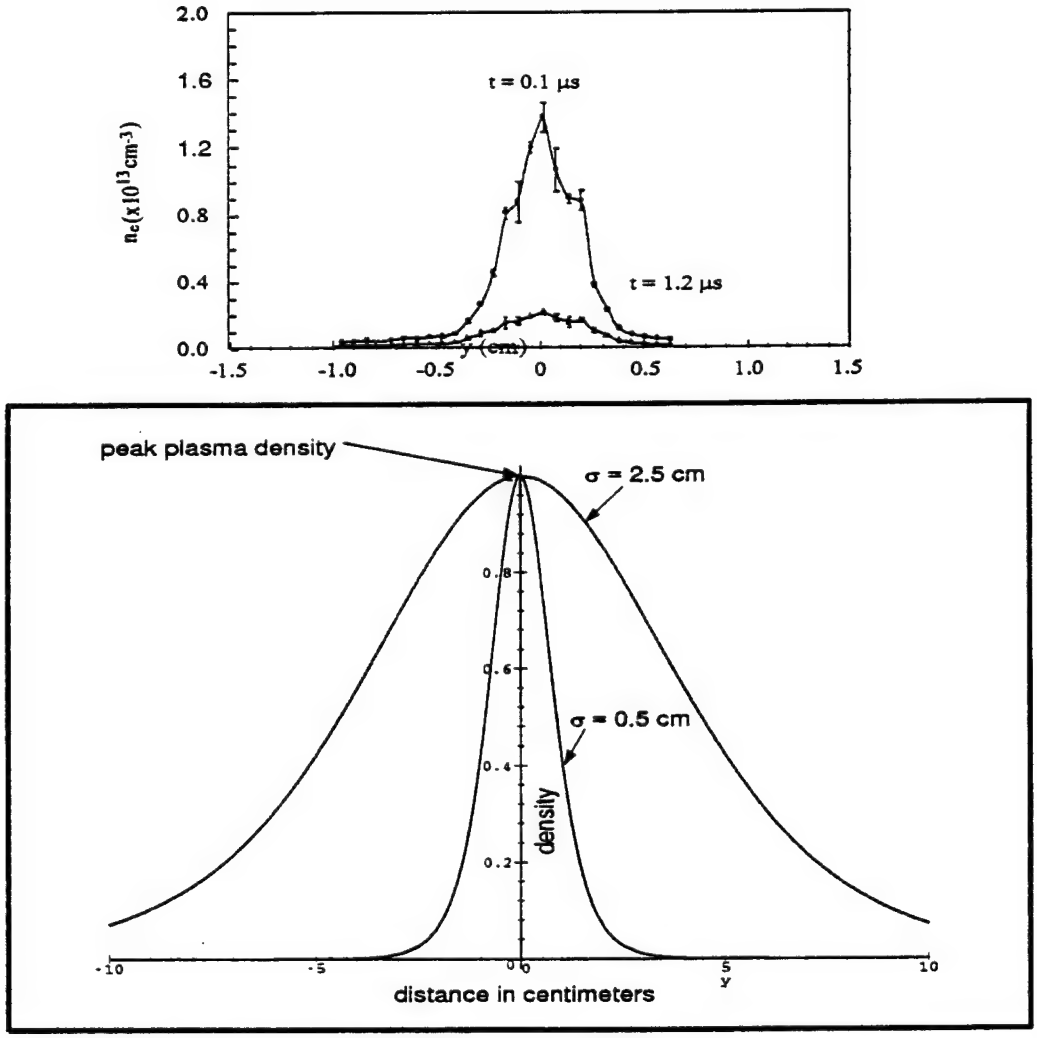

Figure 6: Plasma Density y-profile and Corresponding Epstein Profile

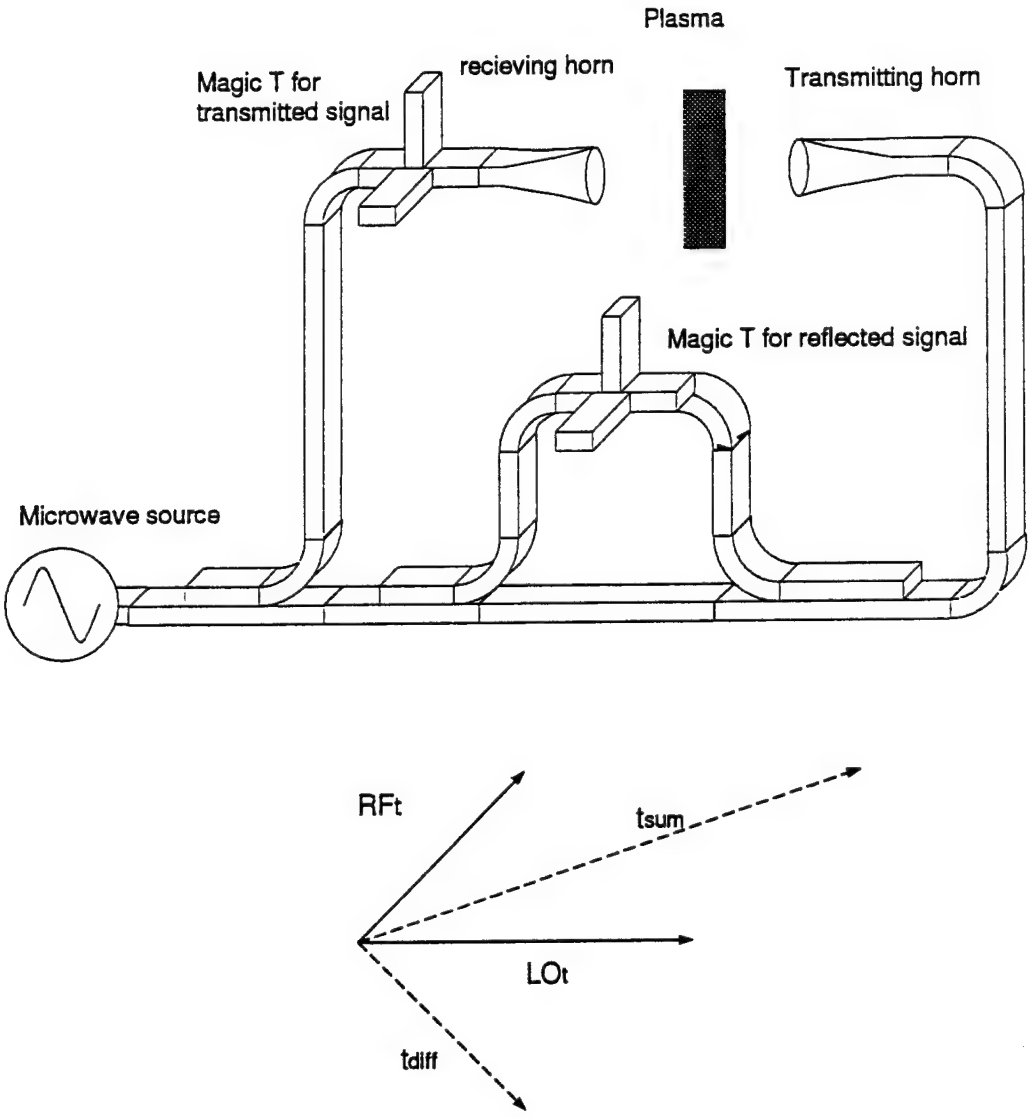

Figure 7: X-band reflectometer/interferometer to measure reflection/ transmission from/through a plasma along with phasor signal representation.

inserted directly after the first coax to waveguide transition from the generator. Accurate frequency measurements were important primarily to assure that the frequency was not drifting during an experiment. Reflections from microwave components as well as from objects in the lab would change with changes in frequency. It was therefore useful to be able to check the exact frequency during calibration and then after the experiment to make sure it did not drift.

4.4.2 Obtaining amplitude and phase from the circuit.

It is useful to consider the signals in phasor notation. Figure 7 demonstrates this. Before the laser shot, LO_t and RF_t are in phase. After, the laser fires and a plasma is produced, there is a change in both the amplitude and phase of RF_t. To obtain the phase of the transmitted signal, ϕ_T,

$|RF_t|$ is first solved for:

$$|RF_t| = \sqrt{{t_{sum}}^2/2 + {t_{diff}}^2/2 - {LO_t}^2}. \tag{30}$$

The phase of the transmitted signal is then found with the law of cosines

$$\phi_T = \pi - cos^{-1}\left(\frac{t_{sum}^2 - |RF_t|^2 - {LO_t}^2}{-2|RF_t|LO_t}\right). \tag{31}$$

Another method is to use t_{mag} to find $|RF_t|$ directly and then find ϕ_T. This would require that the charactaristics of the t_{mag} and MT_t crystals are carefully measured with the same source at the same time. Since there was no convinient way to do that, only t_{diff} and t_{sum} were used to obtain quantitative information about RF_t.

For reflected signals, an aluminum sheet is placed in the position of the laser beam which is where the plasma would be. Then the phase and magnitude of LO_r are adjusted similar to LO_t. That is, r_{diff} is adjusted to be finite and nonzero, but also minimum. Obtaining the phase and magnitude of reflected signals can then be done in a similar manner as for transmission by replacing all t's in equations (30) and (31) with r's.

4.5 Microwave Heterodyne Detection System.

Another method of obtaining amplitude and phase information is by using a heterodyne detection system. The heterodyne system we used utilized two

microwave sources seperated in frequency by 50 MHz. The second source was a HP 8690B Sweepable generator which was purchased in December 1995. As with the homodyne system, a Magic T is functions as an interferometer. Each of two Magic T's will mix two signals. One of these signals will be the upper frequency common to both T's. On one of the T's the other signal will be a reference which does not pass through the plasma. The output on this diode is just a 50 MHz signal with a phase that can be adjusted with a phase shifter. The other T will detect the signal which has traveled through the plasma. The output on its diode will be a 50 MHz signal with a time varying amplitude and a time dependent phase. For the purposes of analysis, it is necessary to assume that the phase shift is a constant over one period of the intermediate frequency (IF). This assumption places a limit on the time response of the system. The two signals are compared. This method is superior in the fact that Fourier transform techniques can be used to filter all but the 50 MHz signal. In addition, the phase of the reflected signal is a directly measurable quantity. The shortcoming of this procedure is a much slower time response if phase is to be known with a high degree of accuracy. This is caused by limitations with the oscilliscope sampling rate. Figure 7

For example, let the sampling rate of the scope be denoted by SF. The number of data points upon which one can accurately measure the phase is just:

$$n = \frac{SF}{IF} \tag{32}$$

However, the error by which the phase is known is given by

$$\Delta\phi = 2\pi\frac{IF}{SF} = 2\pi\frac{1}{n} \tag{33}$$

From this expression it is easy to see that the more accurate determination of ϕ correxponds to a larger IF. But a larger number of data points corresponds to a smaller IF This was a determining factor in choosing 50 MHz for our intermediate frequency. It allowed us to get time resolution of 20 nanoseconds and a determination of the phase to within 6^0.

4.5.1 Obtaining amplitude and phase from the circuit.

The analysis of data is much less cumbersome with the heterodyne system. The amplitude of the reflected signal is simply the Fourier amplitude of the 50 MHz signal on the diode. A Fourier analysis package was employed with

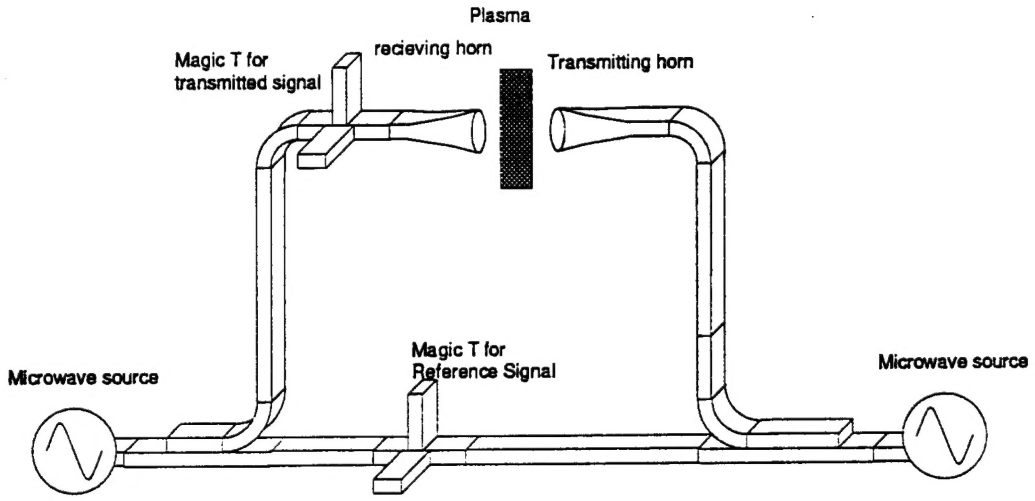

Figure 8: X-band heterodyne detection system.

the the use of our computing facilities The phase of the reflected signal can be found using the reference diode. Before the experiment begins, a phase shifter is used to adjust the reference signal to match the phase of a signal being reflected off an aluminum sheet. This will be assumed to be 180^0. During a typical laser shot there will be a time delay (Δt) between the reference signal and the signal being reflected from the plasma interface. The phase of the reflected signal is given by:

$$\phi = \pi - IF\Delta t \tag{34}$$

5 Acknowledgements

The author wishes to thank Professor John Scharer for supervising this project, Mike Bettenhausen, Yiannis Mouzzouris, and Nguyen Lam for their assistance in computational models, graduate student Guowen Ding for his lab work, and Dmitry Sinitsyn and Stephan Fusi for their lab assistance.

6 Journal Publications

- Shen W., J. E. Scharer, N. T. Lam, B. G. Porter, K. L. Kelly, "Properties of an XUV Laser Created plasma sheet for a microwave reflector", *Journal of Applied Physics*, 78, 6974 (1995).

7 Conferences and presentations.

- Kelly, K. L., J. E. Scharer, G. Ding, M. H. Bettenhausen, N. T. Lam, "Microwave Reflections from an VUV Laser Produced Planar Plasma", *APS-DPP conference*, poster session, Denver, CO., November 1996.

- Kelly, K. L., J. E. Scharer, W. Shen, G. Ding, M. H. Bettenhausen, N. T. Lam, "Microwave Reflections from an VUV Laser Produced Planar Plasma", *IEEE-ICOPS conference*, poster session, Boston, MA., June 1996.

- Scharer,J. E., K. L. Kelly, G. Ding, W. Shen, M. H. Bettenhausen, N. T. Lam, D. Sinitsyn, "VUV Laser Plasma Formation and Microwave

Agile Mirror / Absorber", *IEEE-ICOPS conference*, oral presentation, Boston, MA., June 1996.

- Kelly, K. L., J. E. Scharer, W. Shen, M. H. Bettenhausen, N. T. Lam, B. G. Porter, "Microwave reflection from a VUV Laser Produced Plasma Sheet", *APS-DPP conference*, poster session, Louisville, KY., November 1995.

- Porter, B. G., J. E. Scharer, W. Shen, N. T. Lam, K. Kelly, D. Sinitsyn, "Microwave Reflection from an VUV Laser Produced Planar Plasma", *IEEE-ICOPS conference*, poster session, Madison, WI, June 1995.

References

[1] J. A. Stratton. *Electromagnetic Theory.* McGraw-Hill Book Company, Inc., New York and London, 1941.

[2] W. Shen, J. E. Scharer, B. G. Porter, N. T. Lam, and K. Kelly. Properties of an xuv laser created plasma sheet for microwave reflection. *Journal of Applied Physics*, 78:6974, 1995.

[3] R. A. Meger, J.A. Gregor, R.E. Pechacek, R.F.Fernsler, and W.Manheimer. Experimental investigations of the formation of a plasma mirror for high frequency microwave beam. *Physics of Plasmas — APS-DPP1994 special issue*, 1994.

[4] Y. S. Zhang and J. E. Scharer. Plasma generation in an organic molecular gas by an ultraviolet laser pulse. *Journal of Applied Physics*, 73(10):4779, 1993.

[5] Sin-Li Chen and T. Sekiguchi. Instantaneous direct-display system of plasma parameters by means of a triple probe. *Jounal of Applied Physics*, 36(8):2363, 1965.

AFOSR-TR-97

REPORT DOCUMENTATION PAGE

0577

1. AGENCY USE ONLY (Leave blank)	2. REPORT DATE	3. REPORT TYPE AND DATES COVERED
		FINAL REPORT - 01 Aug 93 - 31 July 97

4. TITLE AND SUBTITLE
(AASERT-93) MICROWAVE ABSORPTION AND REFLECTION FROM ULTRAVIOLET LASER AND ELECTRON CYCLOTRON RESONANCE PRODUCED PLASMAS

5. FUNDING NUMBERS
61103D
3484/TS

6. AUTHOR(S)
Professor John E. Scharer

7. PERFORMING ORGANIZATION NAME(S) AND ADDRESS(ES)
Dept of Electrical and Computer Engineering
University of Wisconsin-Madison
1415 Engineering Drive
Madison, WI 53706-1691

8. PERFORMING ORGANIZATION REPORT NUMBER

9. SPONSORING/MONITORING AGENCY NAME(S) AND ADDRESS(ES)
AFOSR/NE
110 Duncan Avenue Suite B115
Bolling AFB DC 20332-8050

10. SPONSORING/MONITORING AGENCY REPORT NUMBER
F49620-93-1-0465

11. SUPPLEMENTARY NOTES

12a. DISTRIBUTION/AVAILABILITY STATEMENT
APPROVED FOR PUBLIC RELEASE: DISTRIBUTION UNLIMITED

12b. DISTRIBUTION CODE

13. ABSTRACT

This report contains information regarding progress on experiments associated with microwave reflection, absorbtion, and transmission with a laser produced plasma sheet. The progress report is in response to AFOSR AASERT Award F49620-93-1-0465.

The objective of this research is to create a laser produced plasma with a high enough density to reflect or absorb microwaves. The plasma acts as an inertialess reflective or absorptive surface which can be used as an agile mirror in the reflective case, or as a cloaking shield in the absorptive case.

During the past year a new laser was purchased to assist in the research. The new laser installation was accomplished in August 1996. A new heterodyne detection system was also studied to see its benefits as compared to a homodyne system used previously. The National Instruments data acquisition package LabView 4.0.1 was purchased for better interaction with Tektronix oscilliscopes. A new LabView driver was programmed into an updated PowerMac computer.

14. SUBJECT

R OF PAGES

E. PRICE CODE

17. SECURITY CLASSIFICATION OF REPORT	18. SECURITY CLASSIFICATION OF THIS PAGE	19. SECURITY CLASSIFICATION OF ABSTRACT	20. LIMITATION OF ABSTRACT
UNCLASSIFIED	UNCLASSIFIED	UNCLASSIFIED	